Imaginex International Journal of Interdisciplinary Research and Reviews (IIJIRR)
Volume 1, Issue 3, November – December 2026
ISSN: 3140-0094 (Online)
www.iijirr.com

Grip-Force Requirements of Soft-Padded Parallel Grippers in Robotic Pick-and-Place: Load-Dependent Pad Friction, Torsional Slip and Transport Accelerations

S. Sivabalan[1,*], G. Sathish Kumar[1], R. Sridhar[1]

[1]Department of Mechanical Engineering, Vels Institute of Science, Technology and Advanced Studies (VISTAS), Pallavaram, Chennai 600117, Tamil Nadu, India
[*]Corresponding author: S. Sivabalan (e-mail: sivabalan.se@vistas.ac.in)

Abstract

Parallel grippers with elastomer pads are usually sized with a Coulomb rule that treats the pads as point contacts with a constant friction coefficient. This paper tests that rule with a validated model of soft-pad grasping that combines Hertz contact, a two-term friction law (an interfacial shear strength plus a pressure term), the exact friction limit surface of force and torsional moment, and the loads of a robot pick-and-place motion. The model reproduces exact results to within 2×10^{-5}. The twisting moment of an off-centre object, not its weight, usually sets the grip force. A 0.5 kg object held 40 mm off centre needs 6.1 to 11 times the force given by the Coulomb rule, and an offset of only 3.4 mm doubles the requirement for a dome pad on a rough surface. The effective friction coefficient of a smooth dome pad falls from 4.8 at 1 N to 1.0 at 100 N, so a coefficient measured at one load is not valid at another. In a pick-and-place cycle the peak occurs during upward accelerations and, for long objects, during yaw, where it exceeds the Coulomb rule by 28% even for a centred grasp. Scheduling the grip force with the motion lowers the mean force of an off-centre grasp by 27–58%, and making downward accelerations exceed upward ones by $2g$ lowers the peak by 8–20% at the same cycle time. The exact limit surface lies up to 6.6% inside the common ellipse approximation. Pad design guidelines are given.

Keywords: Robotic grasping, parallel gripper, elastomer pad, soft-finger contact, friction limit surface, torsional friction, grip force, pick-and-place

1. Introduction

Most robots in factories, warehouses and farms still pick objects with a simple parallel gripper: two fingers that close on the object, often fitted with elastomer pads [1, 2]. The pads add friction and conform to the object, which is also the idea behind many soft grippers [3–5]. Every such gripper must be told how hard to squeeze. With too little grip force the object slips or falls. With too much it is marked or crushed, the actuator is oversized, and energy is wasted.

In practice the grip force is sized with a Coulomb point-contact rule. The two pads must carry the weight and the inertial force of the object, so each pad needs a normal force of at least $m(g + a)/(2\mu)$, which is then multiplied by a safety factor. The rule hides two assumptions that do not hold for elastomer pads. First, it treats the friction coefficient μ as a constant. For a smooth elastomer pad on a smooth object, the friction force is close to a shear strength times the real contact area [6–8]. That area grows more slowly than the load, so the effective friction coefficient falls as the grip force rises [9, 10]. Second, the rule considers only forces. When the centre of mass (COM) of the object is not on the line through the two contacts, the weight and the inertial forces twist the object about that line. The only thing that resists this twist is the torsional friction of the pads [11, 12]; two point contacts cannot resist it at all [13, 14].

People handle both effects without thinking. They raise their grip force with the torque on a held object, and more so on strongly curved surfaces that give small contact areas [15, 16], and they change the grip force in step with the load force while they move the arm [17]. Robots seldom do. The mechanics needed to size the grip force in these cases exist in pieces: limit-surface models of soft contacts [11, 18, 19], friction laws for elastomers [6, 9, 20], and models of robot trajectories [21, 22]. They have been combined for in-hand pivoting control [23, 24], and pad friction has been measured for gripper design [25]. They have not yet been used together to size the grip force of a gripper over a pick-and-place cycle, or to show how far the Coulomb rule is from what is needed.

This paper fills that gap with a validated numerical model. Its contributions are as follows:

- A limit-surface model of an elastomer pad contact with a two-term friction law (an interfacial shear strength plus a pressure term), for dome pads in Hertz contact and for flat pads. Its integrals agree with exact results and with adaptive quadrature to within 2×10^{-5}. It shows that the exact limit surface lies up to 6.6% inside the common ellipse approximation, so the ellipse errs on the unsafe side.

- A solver for the minimum grip force of a two-pad gripper under any wrench, with the loads computed from the motion of the robot, including yaw rotation of the gripper.
- A quantification of the grip force actually needed. A 0.5 kg object held 40 mm off centre needs 6.1 to 11 times the force given by the Coulomb rule, and an offset of only 3.4 mm doubles the requirement for a dome pad on a rough surface.
- A pick-and-place case study. It shows where in the cycle the peak occurs, that a grip force scheduled with the motion would cut the mean grip force of an off-centre grasp by 27–58%, and that making the downward accelerations exceed the upward ones by $2g$ lowers the peak by 8–20% without changing the cycle time.
- A pad design chart and a set of design guidelines.

Section 2 reviews related work. Section 3 describes the model and Section 4 its numerical solution and validation. Section 5 presents the results, Section 6 discusses them and states the limitations, and Section 7 concludes.

2. Related Work

2.1. Grasp forces and soft-finger contact

Classical grasp analysis models each finger contact as a point contact with or without friction, or as a soft finger that can also transmit a moment about the contact normal [13]. On this basis, grasp forces can be optimised for multi-fingered hands [26], and grasps can be synthesised and ranked by quality measures [27, 28]. Cutkosky related grasp models to the design of hands for manufacturing [14], and Cutkosky and Wright showed that soft fingertips improve both friction and stability [29]. Bicchi argued for simple hands that rely on such robust contact behaviour [30]. Xydas and Kao described the contact of a soft finger by a power law between contact radius and normal force and derived its friction limit surface [11]. Kao and Yang added contact stiffness [12], and Inoue and Hirai proposed an elastic model of a deformable fingertip [31]. Mindlin's analysis of tangential loading, in which slip starts at the edge of the contact, explains the partial slip that precedes gross sliding [32].

2.2. Limit surfaces

For a planar contact, the set of tangential forces and moments that can be carried without sliding is bounded by a limit surface. Goyal et al. derived its properties from the pressure distribution and the friction law and used it to predict sliding motion [18, 33]. Howe and Cutkosky gave practical force–motion models and proposed an ellipsoid as a simple approximation [19], and Zhou et al. fitted convex polynomial models to measured sliding data [34]. Limit surfaces of soft pads are used in tactile control of in-hand object rotation and pivoting [23, 24]. These studies use a constant friction coefficient, and their aim is control or motion prediction, not the sizing of the grip force.

2.3. Friction of elastomers and finger pads

The friction of polymers and elastomers is not Coulombic. Briscoe and Tabor described it by an interfacial shear strength that rises linearly with contact pressure, which gives a friction force with an area term and a load term [9]. Persson developed a theory of rubber friction on rough surfaces [20], Vorvolakos and Chaudhury measured the kinetic friction of silicone rubbers [7], and Chateauminois and Fretigny resolved local friction stresses at a sliding elastomer contact [8]. Adhesion enlarges the contact of soft solids at low load [35]. Sahli et al. showed that, for smooth elastomer and fingertip contacts on glass, static friction equals a constant shear strength times the real contact area at the onset of sliding, and that this area shrinks under shear by up to 30% before sliding starts [6]. The same two-term picture describes the friction of human finger pads [10, 36]: the friction coefficient of skin falls as the load rises [37], and the contact area of the finger pad grows sub-linearly with load [38]. Material data for silicone elastomers used in soft robots are collected in [39, 40].

2.4. Grip force in robots and in humans

Industrial grippers are reviewed in [1], grippers for agricultural robots in [2], and soft grippers in [3–5]. Kargar and Berselli measured the friction of flat and textured silicone pads at loads up to 2 N and proposed a friction stability index; torsion and robot motion were outside their scope [25]. Slip detection and friction estimation with tactile sensors are reviewed in [41, 42]. In humans, grip force rises with the tangential torque on the object [15, 16] and follows the load force predictively during arm movements [17]. Robot trajectories for pick-and-place are usually planned for time, jerk or energy [21, 22, 43], not for the grip force they demand. Table 1 places this paper among the closest studies.

3. Model

3.1. Gripper, object and frames

A parallel gripper holds a rigid object between two pads (Figure 1). The gripper frame has its origin at the grasp centre, midway between the two contact centres. Its y_g axis, the grasp axis, passes through both contacts and is

horizontal; z_g points up and x_g completes the frame. Pad 1 touches the object at $y_g = +w/2$ and pad 2 at $y_g = -w/2$, where w is the grasp width. The object has mass m and inertia tensor $\mathbf{I}$ about its COM, which sits at $\mathbf{r}_C = (e, 0, -h)$ in the gripper frame: e is the horizontal offset along x_g and h the depth of the COM below the grasp axis. The gripper moves with the acceleration of the grasp centre and may rotate about the vertical (yaw). The motion is slow enough for the pads to stay in quasi-static contact, so the question at each instant is whether the friction at the two pads can supply the wrench needed to move the object.

Table 1. Scope of the closest studies and of this paper.

Study	Contact model	Friction law	Torsion about the normal	Robot or hand motion	Main output
Xydas and Kao [11]	Soft finger, power-law contact	Coulomb	Limit surface	No	Contact model, tests
Howe and Cutkosky [19]	General pressure distribution	Coulomb	Limit surface	No	Force–motion models
Costanzo et al. [23, 24]	Soft pads	Coulomb	Limit surface	In-hand pivoting	Tactile control
Sahli et al. [6]	Smooth sphere on plane	Shear strength × area	No	No	Static friction law
Adams et al. [10]	Finger pad	Two-term	No	No	Review of pad friction
Kargar and Berselli [25]	Flat and textured pads	Measured	No	No	Friction stability
Kinoshita et al., Goodwin et al. [15, 16]	Human finger	–	Measured	Hand-held	Grip–torque coupling
This paper	Dome (Hertz) and flat pads	Two-term	Exact limit surface	Pick-and-place with yaw	Grip-force sizing, design rules

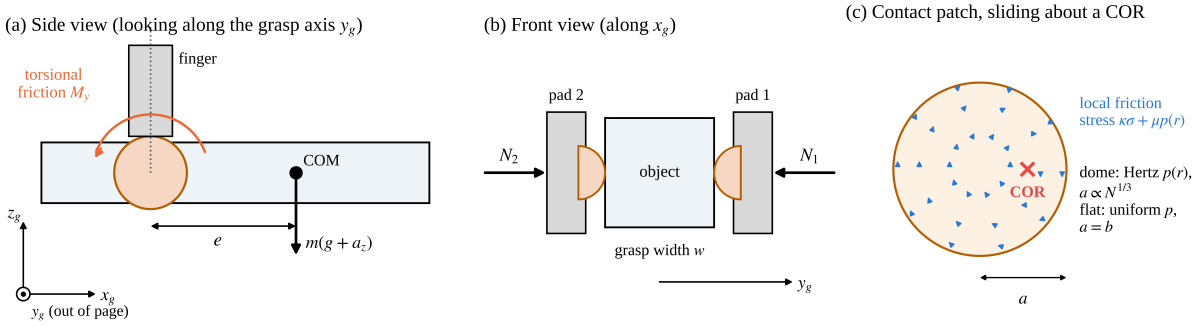

Figure 1. Model. (a) Side view: an object held off centre by the offset *e* tends to rotate about the grasp axis, and only the torsional friction of the pads resists this. (b) Front view: two pads press on the object with normal forces N_1 and N_2. (c) Contact patch of radius *a*: when the object slides by rotating about an instantaneous centre of rotation (COR), the local friction stress opposes the local sliding direction.

3.2. Pad contact

Two pad shapes are considered. A dome pad is an elastomer cap of crown radius R pressed on a flat, rigid face of the object. Its contact follows Hertz theory, with contact radius and pressure

$$a = (3NR / 4E^*)^{1/3}, \quad p(r) = (3N / 2\pi a^2)\,(1 - r^2/a^2)^{1/2} \tag{1}$$

where N is the normal force and $E^* = E/(1 - \nu^2)$ the contact modulus of the pad, the object being much stiffer. The same equations hold for a flat pad on a spherical object of radius R. A flat pad is a circular pad of radius b in full contact with a flat face, modelled with uniform pressure $N/(\pi b^2)$. The contact area of a dome pad grows with $N^{2/3}$; that of a flat pad does not grow at all.

3.3. Friction law

Following Briscoe and Tabor [9], the local shear stress at which the pad slides is taken as the sum of an interfacial shear strength and a pressure term,

$$\tau_f(r) = \kappa\sigma + \mu p(r) \tag{2}$$

The first term dominates for smooth elastomer on a smooth face: Sahli et al. measured $\sigma = 0.36$ MPa for smooth PDMS spheres on glass and showed that static friction is σ times the real contact area at the onset of sliding [6]. Because that area shrinks under shear by up to 30% before sliding starts, the factor κ (1 by default; 0.85 and 0.7 in Section 5.6) scales the adhesive term. The second term is the Coulomb-like behaviour of rough or textured contacts, in which the real contact area grows in proportion to the load [20]. Integrating Eq. (2) over the contact gives the largest tangential force and the largest torsional moment about the contact normal. For a dome pad,

$$T_{\max} = \kappa\sigma\pi a^2 + \mu N, \qquad M_{\max} = (2\pi/3)\,\kappa\sigma a^3 + (3\pi/16)\,\mu N a \tag{3}$$

and for a flat pad $T_{\max} = \kappa\sigma\pi b^2 + \mu N$ and $M_{\max} = (2/3)b\,T_{\max}$. The effective friction coefficient $T_{\max}/N$ of a smooth dome pad therefore falls as $N^{-1/3}$, while its torsional capacity per newton, $M_{\max}/N = \pi\kappa\sigma R/(2E^*)$, does not depend on the load. For a rough dome pad the opposite holds: the friction coefficient is constant, but the torsional capacity per newton grows with the contact radius, as $N^{1/3}$.

Four reference pads are studied (Table 2). All are made of PDMS with $E = 1.6$ MPa and $\nu = 0.5$ [6]. The three dome pads have $R = 25$ mm, close to the 24.81 mm caps of [6]. They differ in the face they grip. On a smooth face (DS) friction is purely adhesive, with $\sigma = 0.36$ MPa and $\mu = 0$. On a rough face (DR) it is purely Coulombic, with $\sigma = 0$ and $\mu = 1$. The mixed case (DM) has half of each, $\sigma = 0.18$ MPa and $\mu = 0.5$. The value $\mu = 1$ is a nominal one of the order found for rubber on rough hard surfaces [20]. It is also the value used in the Coulomb rule throughout, so the rough dome pad and the rule agree when no torsion acts. The flat pad (FR) has $b = 10$ mm and $\mu = 1$. With N between 1 and 100 N the dome contact radius stays between 2.1 and 9.6 mm, so $a/R \le 0.38$; Hertz theory is commonly accepted up to $a/R \approx 0.4$, and this limit is marked in the design chart of Section 5.6.

Table 2. Model parameters and reference cases.

Quantity	Value	Source or reason
Pad material: modulus E, Poisson ratio ν	1.6 MPa, 0.5 (PDMS)	Measured in [6]
Dome crown radius R; flat pad radius b	25 mm; 10 mm	Caps of 24.81 mm in [6]; design choice
Shear strength σ, smooth face (DS)	0.36 MPa	PDMS on glass [6]
Pressure coefficient μ, rough face (DR, FR)	1.0	Nominal value [20]
Mixed face (DM)	$\sigma = 0.18$ MPa, $\mu = 0.5$	Half of each term
Contact-area factor κ	1 (0.85 and 0.7 in Section 5.6)	Area loss under shear [6]
Coulomb rule	$\mu = 1$, point contacts, no torsion	Common sizing practice
Object	0.5 kg bar, 200 × 30 × 30 mm; also 0.25 and 1 kg	Typical machined part
Grasp width w; COM offset e	30 mm; 0–60 mm	Grasp across the bar
Pick-and-place path	Lift 0.10 m, transfer 0.40 m with 90° yaw, lower 0.10 m	Section 3.6
Peak accelerations	3–15 m/s^2	Collaborative to industrial robots

3.4. Limit surface

When the object slides on a pad, the motion of the contact patch is a rotation about an instantaneous centre of rotation (COR) in the contact plane; pure translation is the limit of a COR at infinity. Placing the COR at $(\rho, 0)$ and taking the friction stress at each point opposite to the local sliding direction gives the tangential force and the torsional moment

$$T(\rho) = \left|\int \tau_f\,(x-\rho)/d\;\mathrm{d}A\right|, \qquad M(\rho) = \left|\int \tau_f\,[x(x-\rho)+y^2]/d\;\mathrm{d}A\right| \tag{4}$$

with $d = [(x-\rho)^2 + y^2]^{1/2}$. As ρ runs from 0 to infinity, (T, M) traces the limit surface from pure torsion ($T = 0$, $M = M_{\max}$) to pure sliding ($T = T_{\max}$, $M = 0$) [18]. Since Eq. (2) is the sum of a uniform term and a term with the Hertz pressure shape, each limit surface is the sum of two normalised shapes, one for uniform and one for Hertz stress, each scaled by its own maximum from Eq. (3). The two normalised shapes are computed once, on a polar grid of the unit disc. A load (T, M) is carried without gross slip if it lies inside the limit surface. The widely used ellipse approximation replaces the surface by $(T/T_{\max})^2 + (M/M_{\max})^2 = 1$ [11, 19].

3.5. Two-pad grasp and minimum grip force

Let $\mathbf{F} = (F_x, F_y, F_z)$ and $\mathbf{M} = (M_x, M_y, M_z)$ be the force and the moment about the grasp centre that the two pads must apply to the object, in the gripper frame. Since both contact centres lie on the grasp axis, the normal forces carry

F_y, the tangential forces carry F_x, F_z, M_x and M_z, and the torsional moments of the pads alone carry M_y. Static equilibrium fixes the tangential forces of pads 1 and 2 and their normal forces:

$$\mathbf{t}_{1,2} = (F_x/2 \mp M_z/w,\ F_z/2 \pm M_x/w), \qquad N_{1,2} = N \mp F_y/2 \tag{5}$$

where N is the mean grip force set by the gripper. The split of M_y between the two pads is not fixed by statics. The grasp holds if a split exists that keeps both pads inside their limit surfaces, that is, if

$$|\mathbf{t}_i| \le T_{max}(N_i) \ \ (i = 1, 2) \quad \text{and} \quad |M_y| \le M_{av}(N_1, |\mathbf{t}_1|) + M_{av}(N_2, |\mathbf{t}_2|) \tag{6}$$

where $M_{av}(N, T)$ is the largest moment on the limit surface at tangential force T. Both pad limit surfaces grow with the normal force, so the minimum grip force N_{min} is found by bisection. The Coulomb rule used for comparison treats the pads as point contacts with $\mu = 1$ and ignores M:

$$N_C = (F_x^2 + F_z^2)^{1/2} / 2\mu + |F_y|/2 \tag{7}$$

Several cases have closed-form solutions, which are used to check the solver and explain the results. Under pure torsion M_y, the smooth dome pad needs $N_{min} = M_y E^*/(\pi\kappa\sigma R)$, the flat pad needs $N_{min} = 3M_y/(4\mu b)$, and the rough dome pad needs $N_{min} \propto M_y^{3/4}$. Under a pure tangential load F_z, the rough dome pad needs $F_z/(2\mu)$, equal to the Coulomb rule, while the smooth dome pad needs only $N_{min} = (4E^*/3R)[F_z/(2\pi\kappa\sigma)]^{3/2}$.

3.6. Loads from the robot motion

For a grasp-centre acceleration $\mathbf{a}$, yaw angle ψ, yaw rate $\boldsymbol{\omega}$ and yaw acceleration $\boldsymbol{\alpha}$, the COM acceleration is $\mathbf{a}_C = \mathbf{a} + \boldsymbol{\alpha} \times \mathbf{r} + \boldsymbol{\omega} \times (\boldsymbol{\omega} \times \mathbf{r})$, with $\mathbf{r}$ the COM offset rotated into the world frame, and the wrench on the object is

$$\mathbf{F} = m(\mathbf{a}_C - \mathbf{g}), \qquad \mathbf{M} = \mathbf{I}_w\boldsymbol{\alpha} + \boldsymbol{\omega} \times \mathbf{I}_w\boldsymbol{\omega} + \mathbf{r} \times \mathbf{F} \tag{8}$$

which is then rotated into the gripper frame. Each move of length D is a rest-to-rest motion with smooth acceleration pulses, $a_1 \sin^2(\pi t/T_1)$ followed by $-a_2 \sin^2(\pi t/T_2)$. The peak speed is $v_{max} = [D/(1/a_1 + 1/a_2)]^{1/2}$ and $T_i = 2v_{max}/a_i$, so the move time depends only on $1/a_1 + 1/a_2$. The case-study cycle lifts the object by 0.10 m, transfers it by 0.40 m while the gripper yaws by 90°, and lowers it by 0.10 m, with 50 ms pauses between the moves. In the lift, the upward acceleration a_{up} comes first and the downward deceleration a_{down} second; in the lowering the order is reversed. Unless stated otherwise $a_{up} = a_{down} = a$.

4. Numerical Method and Validation

4.1. Numerical method

The two normalised limit-surface shapes were computed with a midpoint rule on a polar grid of 800 radial by 1600 angular cells of the unit disc, at 642 COR positions ($\rho/a = 0$ and 641 values spaced logarithmically from 10^{-4} to 10^{4}), and stored as tables. For a given pad and normal force, the limit surface is the scaled sum of the two tables, and M_{av} follows by linear interpolation. The minimum grip force was found by bisection to a relative tolerance of 10^{-6}. The case-study cycle was evaluated every 2 ms. The model was written in Python 3 with NumPy and SciPy; the whole study, including the tables, runs in under one minute on a desktop computer.

4.2. Validation

Table 3 summarises the checks. The integrals of the stress fields and of their first moments agree with the exact values to within 2×10^{-5}; refining the grid to 1600 × 3200 cells changes the normalised limit surface by less than 4×10^{-6}; and an independent adaptive quadrature (SciPy dblquad) agrees with the grid result to within 6×10^{-6} at four COR positions for both stress shapes. The solver reproduces all six closed-form cases of Section 3.5 to within 1×10^{-6}. The wrench of Eq. (8) matches a finite-difference derivative of the linear and angular momentum of a rotating, offset object to within 5×10^{-9}, and the motion profiles reach their target distance with zero end velocity.

The same computation tests the ellipse approximation. The exact limit surface lies inside the ellipse everywhere except at its two ends. Its smallest normalised radius is 0.934 for uniform stress (at a COR at $\rho/a = 0.77$) and 0.940 for Hertz stress (at $\rho/a = 0.69$): under combined force and moment, the exact surface lies up to 6.6% and 6.0% inside the ellipse. The ellipse therefore errs on the unsafe side; its effect on the grip force is shown in Section 5.2.

5. Results

5.1. Pad friction and torsional capacity

Figure 2(b) shows how strongly the friction of the smooth dome pad depends on the load. Its effective friction coefficient is 4.82 at a normal force of 1 N, 2.24 at 10 N and 1.04 at 100 N, and that of the mixed pad falls from 2.91 to 1.02. A friction coefficient measured at one load is therefore not valid at another. Figure 2(c) shows the twisting moment each pad can carry per newton of normal force. It is 6.63 mm for the smooth dome pad and 6.67 mm for the flat pad at every load. For the rough dome pad it grows with the contact radius, from 1.22 mm at 1 N to 2.62 mm at 10 N and 5.64 mm at 100 N. At the same normal force, a rough dome pad therefore resists a twist much less

well than a smooth one, and the gap is largest at the low forces at which grippers usually work. Figure 2(a) shows the normalised limit surfaces: the shapes for uniform and Hertz stress are close to each other, and both lie inside the ellipse approximation.

Table 3. Validation of the model. The last column gives the largest relative error (absolute for the normalised limit surface and the motion profiles).

Check	Reference	Largest error
Stress integrals $\int\tau\,dA$, $\int\tau r\,dA$ (uniform, Hertz)	Exact: π, $2\pi/3$; $2\pi/3$, $\pi^2/8$	1.9×10^{-5}
Grid refinement 800 × 1600 → 1600 × 3200	Change in T/T_{max}, M/M_{max}	3.9×10^{-6}
Adaptive quadrature at ρ/a = 0.3, 0.7, 1.5, 3	SciPy dblquad	5.1×10^{-6}
Rough dome, tangential load	Closed form, N_{min} = 4 N	$< 10^{-12}$
Smooth dome, tangential load	Closed form, N_{min} = 0.7568 N	2.0×10^{-7}
Smooth dome, pure torsion	Closed form, N_{min} = 15.09 N	2.3×10^{-7}
Rough dome, pure torsion	Closed form, N_{min} = 27.31 N	4.6×10^{-7}
Flat pad, pure torsion	Closed form, N_{min} = 15 N	$< 10^{-12}$
Normal-force imbalance only	Closed form, N_{min} = 1.5 N	9.5×10^{-7}
Wrench of Eq. (8)	Finite-difference momentum rates	4.6×10^{-9}
Motion profiles (0.4 m; 5/5 and 2/8 m/s^2)	Distance 0.4 m, end velocity 0	2.4×10^{-15}

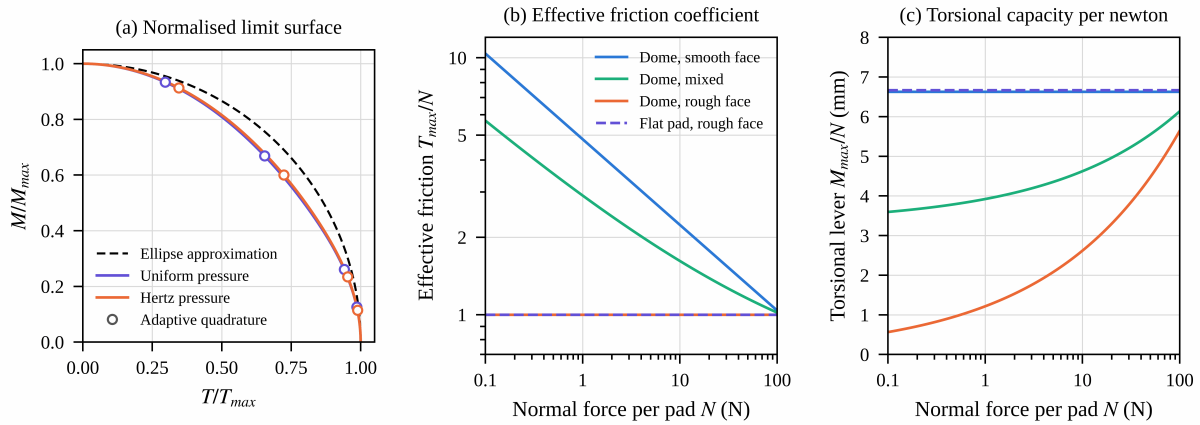

Figure 2. Pad friction. (a) Normalised limit surfaces for uniform and Hertz stress against the ellipse approximation; markers are independent adaptive-quadrature points. (b) Effective friction coefficient T_{max}/N and (c) torsional capacity per newton, M_{max}/N, of the four reference pads.

5.2. Holding at rest: the role of the COM offset

Figure 3(a) shows the minimum grip force for the 0.5 kg bar held at rest, against the COM offset. When the grasp passes through the COM, the rough dome pad and the flat pad need 2.45 N per pad, the same as the Coulomb rule. The smooth and mixed dome pads need only 0.363 N and 0.790 N, so for these pads the rule overestimates the force by factors of 6.8 and 3.1. As soon as the COM is offset, the twisting moment *mge* takes over. The requirement grows almost linearly with the offset, and at e = 40 mm it is 14.9 N for the smooth dome pad, 19.9 N for the mixed one, 27.0 N for the rough one and 15.0 N for the flat pad: 6.1, 8.1, 11.0 and 6.1 times the Coulomb rule. Table 4 gives the offsets at which the requirement reaches two and five times the rule. For the rough dome pad an offset of 3.4 mm is enough to double it, and 13.6 mm to multiply it by five.

Figure 3(b) shows the same results as a ratio to the Coulomb rule for objects of 0.25, 0.5 and 1 kg. For the smooth dome pad the ratio hardly depends on the mass (6.06, 6.07 and 6.09 at e = 40 mm), because both the torsional capacity and the load grow in proportion to the normal force. For the rough dome pad the ratio falls with the mass (13.1, 11.0 and 9.3), because its torsional capacity grows faster than the normal force. Using the ellipse approximation instead of the exact limit surface would have underestimated the required force by up to 8.1% in these cases; the largest errors occur at small offsets, where force and moment are of similar size relative to their maxima.

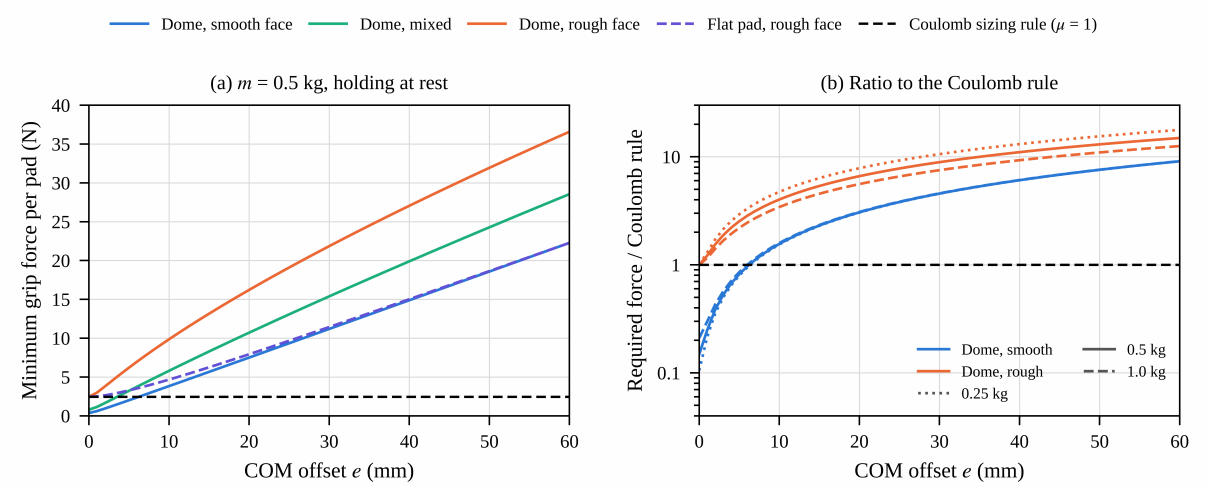

Figure 3. Holding at rest. (a) Minimum grip force per pad against the COM offset for the 0.5 kg bar. (b) Ratio of the required force to the Coulomb rule for objects of 0.25, 0.5 and 1 kg.

Table 4. Minimum grip force per pad (N) for the 0.5 kg bar held at rest, against the COM offset *e*.

COM offset *e* (mm)	Dome, smooth (DS)	Dome, mixed (DM)	Dome, rough (DR)	Flat, rough (FR)	Coulomb rule
0	0.363	0.790	2.45	2.45	2.45
5	2.01	3.22	6.20	3.28	2.45
10	3.83	5.79	9.85	4.66	2.45
20	7.50	10.7	16.2	7.93	2.45
40	14.9	19.9	27.0	15.0	2.45
60	22.3	28.5	36.6	22.3	2.45
Offset for 2 × rule (mm)	12.9	8.3	3.4	10.8	–
Offset for 5 × rule (mm)	32.9	23.3	13.6	32.3	–

5.3. Direction of the acceleration

Figure 4 shows the minimum grip force for an acceleration of 10 m/s^2 in any direction of two planes, and Table 5 lists the values along the axes. With the grasp through the COM, an upward acceleration doubles the requirement of the rough dome pad (4.95 N against 2.45 N at rest) and nearly triples that of the smooth one (1.04 N against 0.363 N), because the smooth pad needs a force that grows with the 3/2 power of the load. A downward acceleration of this size nearly unloads the grasp. An acceleration along the grasp axis is carried by the difference between the two normal forces, so the trailing pad must be squeezed by an extra $ma/2$ = 2.5 N. With the COM 40 mm off the grasp axis, the twisting moment dominates every direction. An upward acceleration again about doubles the requirement (30.1 N for the smooth dome pad, 45.9 N for the rough one), while horizontal accelerations change the requirement of the dome pads by less than 4%; for the flat pad, an acceleration along the grasp axis adds 13%.

This changes when the COM also lies below the grasp axis, as it does when a bar is gripped near its top face. With e = 40 mm and h = 20 mm, a 10 m/s^2 acceleration in the direction of the offset ($+x_g$) adds an inertial moment mha to the gravity moment and raises the requirement by 51% (smooth dome), 36% (rough dome) and 51% (flat pad). The same acceleration in the opposite direction lowers it to 7.46, 16.2 and 8.33 N. The orientation of the grasp relative to the direction of travel therefore matters whenever the COM is below the fingers.

5.4. Pick-and-place case study

Figure 5 follows the 0.5 kg bar through a full pick-and-place cycle with peak accelerations of 15 m/s^2 (cycle time 1.02 s), and Table 6 also gives the results for 5 m/s^2 (1.70 s). With the grasp through the COM, the smooth dome pad never needs more than 4.43 N. For the rough dome pad and the flat pad, the peak of 7.95 N does not occur in the lift, as the Coulomb rule would suggest, but during the transfer, and it is 28% above the peak of the rule (6.22 N). The cause is the yaw of the long bar. A yaw acceleration of up to 59 rad/s^2 needs a moment of 0.10 N·m about z_g, which the pads can supply only through opposite tangential forces of 3.3 N each (Eq. 5), on top of the forces that carry the weight.

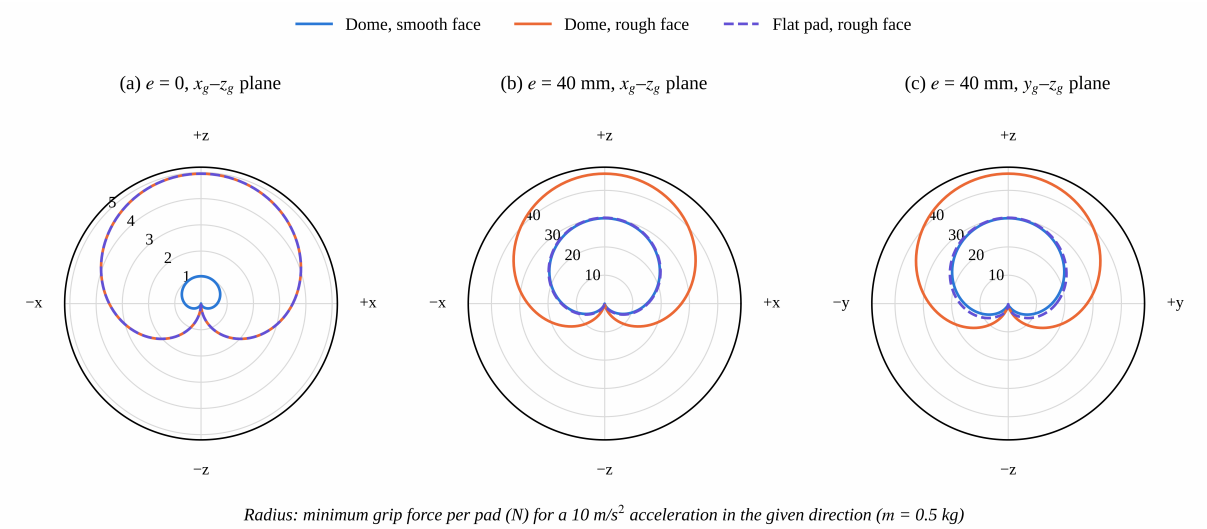

Figure 4. Minimum grip force per pad for a 10 m/s² acceleration of the gripper in each direction of (a, b) the x_g–z_g plane and (c) the y_g–z_g plane, for the grasp through the COM and for a COM offset of 40 mm (0.5 kg bar).

Table 5. Minimum grip force per pad (N) for a 10 m/s² acceleration along the gripper axes (0.5 kg bar).

Acceleration	*e* = 0: DS	*e* = 0: DR	*e* = 40 mm: DS	*e* = 40 mm: DR	*e* = 40 mm: FR	Coulomb rule
At rest	0.363	2.45	14.9	27.0	15.0	2.45
$+x_g$ (across the grasp)	0.620	3.50	15.0	27.2	15.3	3.50
$+y_g$ (along the grasp axis)	2.86	4.95	15.5	27.9	17.0	4.95
$+z_g$ (upward)	1.04	4.95	30.1	45.9	30.3	4.95
$-z_g$ (downward)	0.001	0.048	0.287	1.40	0.291	0.047
$+x_g$, COM 20 mm below axis	–	–	22.5	36.9	22.6	–
$-x_g$, COM 20 mm below axis	–	–	7.46	16.2	8.33	–

The Coulomb rule does not depend on the offset; it is the same for e = 0 and e = 40 mm.

With the COM 40 mm off centre, the picture is dominated by torsion. The requirement never drops below the holding force at rest (14.9 N for the smooth dome pad, 27.0 N for the rough one). It peaks during the upward accelerations, at the start of the lift and at the end of the lowering: 37.8, 54.4 and 38.0 N for the smooth dome, rough dome and flat pads at 15 m/s², against 6.20 N from the Coulomb rule. A gripper sized by the rule with a safety factor of 2 would thus slip in every cycle, with all three pads. The mean requirement over the cycle is much lower than the peak. A grip force scheduled with the planned motion, as people do when they move a hand-held object [17], would reduce the mean grip force by 27–58% compared with a constant force set at the peak, and by 30–76% for the grasp through the COM.

5.5. Shaping the vertical moves

Since the peak occurs in the phases where the object is accelerated upward, the vertical moves can be shaped to reduce it. During an upward acceleration a_{up} the pads carry $m(g + a_{up})$; during a downward acceleration a_{down} they carry $m|g - a_{down}|$. The move time depends only on $1/a_{up} + 1/a_{down}$ (Section 3.6). For a fixed move time, the larger of the two loads is therefore smallest when they are equal, that is when

$$a_{down} = a_{up} + 2g \tag{9}$$

Figure 6 and Table 7 compare this shaping with symmetric moves of the same duration for the off-centre bar. It lowers the peak grip force by 11–20% for the smooth dome pad, 8–15% for the rough one and 11–20% for the flat pad, without changing the cycle time; the gain grows with the acceleration level. The price is a fast downward acceleration, 21.2–29.7 m/s² in these cases, which only some robots can deliver. Even a capped version helps: at 5 m/s², limiting the downward acceleration to 15 m/s² and the upward one to 3 m/s² gives the same cycle time and lowers the peak of the smooth dome pad from 22.5 to 19.5 N (14%).

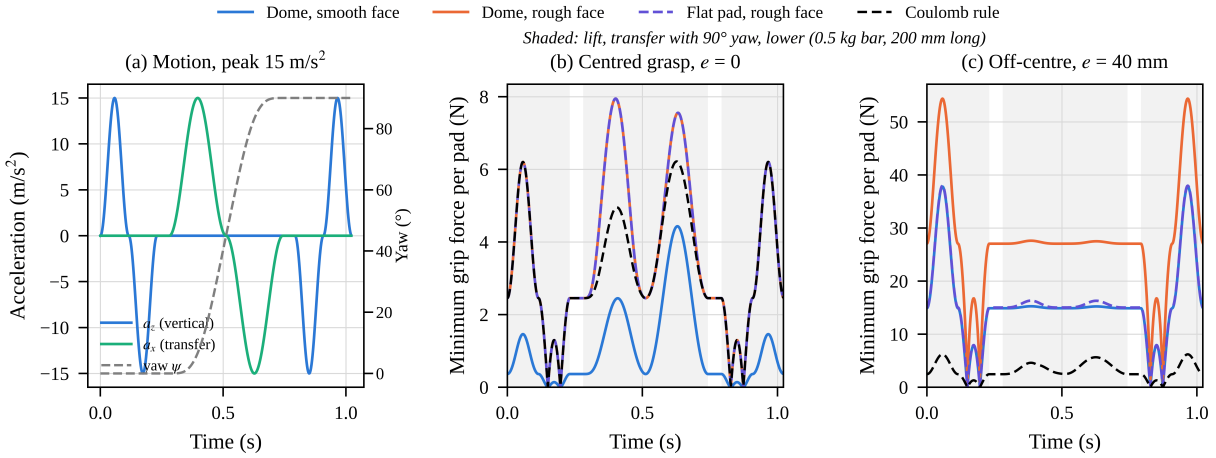

Figure 5. Pick-and-place cycle of the 0.5 kg bar with peak accelerations of 15 m/s². (a) Vertical and transfer accelerations and the yaw angle. (b, c) Minimum grip force per pad for the grasp through the COM and for a COM offset of 40 mm, with the Coulomb rule for comparison. Shaded: lift, transfer with 90° yaw, and lowering.

Table 6. Pick-and-place case study: peak / cycle-mean minimum grip force per pad (N).

Offset, peak acceleration	Cycle time (s)	Dome, smooth	Dome, rough	Flat, rough	Coulomb rule, peak
0, 5 m/s²	1.70	1.65 / 0.560	3.88 / 2.72	3.88 / 2.72	3.70
0, 15 m/s²	1.02	4.43 / 1.08	7.95 / 3.68	7.95 / 3.68	6.22
40 mm, 5 m/s²	1.70	22.5 / 14.9	36.9 / 26.9	22.7 / 15.0	3.70
40 mm, 15 m/s²	1.02	37.8 / 15.9	54.4 / 27.7	38.0 / 16.2	6.20

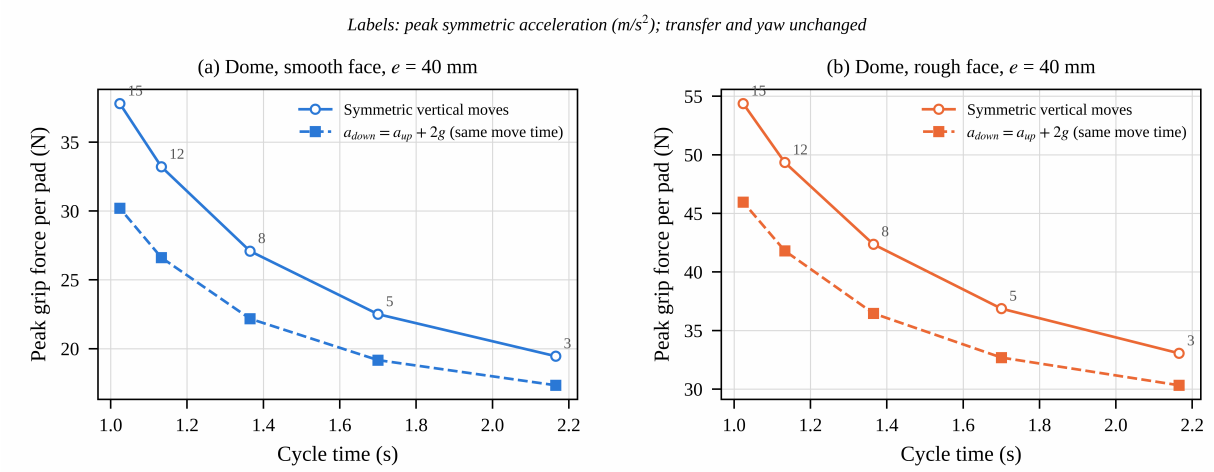

Figure 6. Peak grip force per pad against cycle time for symmetric vertical moves and for moves shaped by Eq. (9) with the same duration (off-centre bar, *e* = 40 mm). Labels give the peak acceleration of the symmetric moves.

5.6. Pad design

Figure 7 maps the minimum grip force for the off-centre bar at rest over the crown radius and modulus of the dome pad, and against the radius of the flat pad. For the smooth dome pad the torsional capacity per newton is $\pi\kappa\sigma R/(2E^*)$, so the required force scales with E/R. At R = 25 mm it rises from 4.65 N for a soft pad (E = 0.5 MPa) to 46.5 N for a stiff one (5 MPa), and at E = 1.6 MPa it falls from 37.2 N for R = 10 mm to 3.72 N for R = 100 mm. For small, stiff domes, however, the contact radius at the required force exceeds 0.4R (shaded), where Hertz theory no longer applies (a/R = 0.51 for R = 10 mm). The rough dome pad is much less sensitive to its design, because its required force scales only with $(E/R)^{1/4}$: 20.3–35.9 N over the same range of moduli and 19.2–34.0 N over the same radii. For the flat pad the requirement falls in inverse proportion to the pad radius, from 29.6 N for b = 5 mm to 7.93 N for b = 20 mm.

Table 7. Peak grip force per pad (N), symmetric → shaped vertical moves with the same cycle time (off-centre bar, e = 40 mm).

a (m/s²)	a_{up} (m/s²)	a_{down} (m/s²)	Cycle time (s)	Dome, smooth	Dome, rough	Flat, rough
3	1.61	21.2	2.17	19.5 → 17.3	33.1 → 30.3	19.6 → 17.5
5	2.81	22.4	1.70	22.5 → 19.2	36.9 → 32.7	22.7 → 19.3
8	4.78	24.4	1.36	27.1 → 22.2	42.4 → 36.5	27.3 → 22.3
12	7.69	27.3	1.13	33.2 → 26.6	49.3 → 41.8	33.4 → 26.8
15	10.04	29.7	1.02	37.8 → 30.2	54.4 → 46.0	38.0 → 30.4

The contact-area factor κ matters for the smooth pad. If the real contact area shrinks under shear before sliding, as observed by Sahli et al. [6], the required force of the off-centre grasp rises by 18% for κ = 0.85 and by 43% for κ = 0.7. For the grasp through the COM, where the requirement scales with $\kappa^{-3/2}$, the rise for κ = 0.7 is 71%. A design for smooth pads should therefore keep this margin.

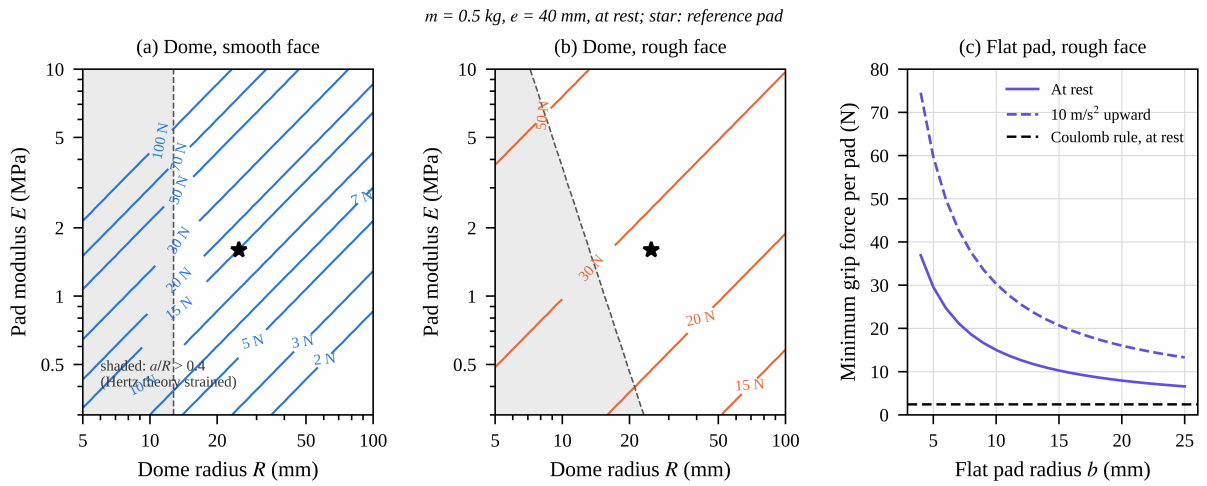

Figure 7. Pad design for the off-centre bar at rest (m = 0.5 kg, e = 40 mm). Minimum grip force per pad (N) over the crown radius and modulus of (a) a smooth dome pad and (b) a rough dome pad; the star is the reference pad and the shaded region has a/R > 0.4. (c) Flat pad, at rest and under a 10 m/s² upward acceleration.

6. Discussion

6.1. Design guidelines

Table 8 condenses the results into guidelines for sizing the grip force and choosing the pads of a parallel gripper. Each guideline is tied to the evidence behind it.

Table 8. Design guidelines drawn from the study.

Situation	Guideline	Evidence
COM off the grasp axis by more than a few millimetres	Size the grip force for the twisting moment, not for the weight; use the closed forms of Section 3.5 for a first estimate	6.1–11 times the Coulomb rule at e = 40 mm (Table 4)
Choice of pad for off-centre objects	Prefer flat pads or large, soft dome pads; avoid small rough domes	Torsional capacity per newton (Figure 2c); design chart (Figure 7)
Smooth elastomer pads	Do not use a friction coefficient measured at another load	Effective friction falls from 4.82 to 1.04 between 1 and 100 N (Figure 2b)
COM below the fingers	Grip at the height of the COM, or travel so that the inertial moment opposes the gravity moment	+51% or −50% for a 10 m/s² horizontal acceleration (Table 5)
Long objects that are yawed	Include the yaw inertia; it loads the pads through opposite tangential forces	28% above the Coulomb rule for a centred grasp (Table 6)

Situation	Guideline	Evidence
Grip force control	Schedule the grip force with the planned motion	Mean grip force 27–58% lower for the off-centre grasp (Table 6)
Vertical moves	Use $a_{down} = a_{up} + 2g$ where the robot allows; otherwise limit the upward accelerations	Peak 8–20% lower at the same cycle time (Table 7)
Margins	Keep a margin for area loss at slip onset and, if used, for the ellipse approximation	+43% for $\kappa = 0.7$; up to 8.1% from the ellipse (Sections 5.2, 5.6)

6.2. Relation to earlier work

The results agree with what is known about human grip. People increase their grip force with the torque on the object, and more steeply when the grasped surface is strongly curved [15, 16]. In the present model a strongly curved surface means a small contact radius and hence little torsional capacity per newton, which is exactly the behaviour of the rough dome pad at low loads (Figure 2c). People also scale their grip force with the load force during a movement, ahead of the load [17], which is the scheduling of Section 5.4. On the robot side, the torsional friction of soft pads is used deliberately to let objects pivot in the grasp [23, 24]; the same mechanics, read the other way, sets the force that prevents unwanted pivoting. The finding that the exact limit surface lies inside the ellipse is consistent with the ellipse being proposed as a practical approximation rather than an exact result [11, 19]. Finally, the strong load dependence of the friction of smooth pads follows directly from the area-based static friction law of Sahli et al. [6] combined with Hertz contact, and agrees with the falling friction coefficient of finger pads and skin under rising load [10, 37].

6.3. Limitations

The model has the limits of a quasi-static contact analysis, and several choices deserve mention.

- Friction is rate-independent. Elastomer friction depends on sliding speed and temperature [7, 20], and static friction may also depend on how long the contact has been held.
- Only gross slip is modelled. Partial slip at the contact edge starts earlier [32] and is what tactile slip sensors detect [41, 42].
- Adhesion is included only through the shear strength. JKR adhesion enlarges the contact at low loads [35] and would lower the requirement of the smooth pad slightly, so the model is conservative there.
- Moments about x_g and z_g are carried only by tangential forces; pads can also resist them through a shift of the contact pressure. The object is rigid and the two pads have equal friction.
- The friction data come from one well-characterised pair, PDMS on glass [6]. Oil, dust or wear can lower the shear strength greatly, and other elastomers will differ. Experiments with an instrumented gripper are needed to confirm the results.

7. Conclusions

This paper sized the grip force of a two-pad parallel gripper with elastomer pads, using a validated model that combines Hertz contact, a two-term friction law, the exact friction limit surface and the loads of a pick-and-place motion. Three findings stand out. First, the twisting moment of an off-centre object, not its weight, sets the grip force: a 0.5 kg object held 40 mm off centre needs 6.1–11 times the force given by the Coulomb rule, and an offset of 3.4 mm doubles the requirement for a rough dome pad. Second, the friction of smooth elastomer pads depends strongly on the load, so a friction coefficient measured at one load cannot be used at another, and the torsional capacity per newton of a pad depends on its shape and stiffness much more than its friction coefficient suggests. Third, the motion matters: the peak occurs during upward accelerations or, for long objects, during yaw, and scheduling the grip force with the motion or shaping the vertical moves by $a_{down} = a_{up} + 2g$ lowers the mean or the peak grip force substantially without lengthening the cycle.

Future work will test these predictions with an instrumented gripper and a six-axis force sensor, extend the friction law to rate and temperature effects, and use the model online to set the grip force from the planned trajectory and an estimate of the COM position.

Declarations

Conflict of interest. The authors declare no known competing financial interests or personal relationships that could have appeared to influence the work reported in this paper.

Funding. This research did not receive any specific grant from funding agencies in the public, commercial, or not-for-profit sectors.

Data availability. The model was written in Python 3 with NumPy and SciPy, and every number reported in this paper comes from it. The equations and all parameter values needed to reproduce the results are given in Sections

3 and 4 and in Table 2. The code and the raw results are available from the corresponding author on reasonable request.

Use of generative AI. During the preparation of this work the authors used Claude (Anthropic) to help draft and edit the text, write and run the Python code, and prepare the figures and tables. After using this tool, the authors reviewed and edited the content as needed and take full responsibility for the content of the publication.

Ethics approval and consent. Not applicable. This is a computational study and involves no human participants, animals or personal data.

References

[1] L. Birglen and T. Schlicht, "A statistical review of industrial robotic grippers," *Robotics and Computer-Integrated Manufacturing*, vol. 49, pp. 88–97, 2018, doi: 10.1016/j.rcim.2017.05.007.

[2] B. Zhang, Y. Xie, J. Zhou, K. Wang, and Z. Zhang, "State-of-the-art robotic grippers, grasping and control strategies, as well as their applications in agricultural robots: A review," *Computers and Electronics in Agriculture*, vol. 177, Art. no. 105694, 2020, doi: 10.1016/j.compag.2020.105694.

[3] J. Shintake, V. Cacucciolo, D. Floreano, and H. Shea, "Soft robotic grippers," *Advanced Materials*, vol. 30, no. 29, Art. no. 1707035, 2018, doi: 10.1002/adma.201707035.

[4] J. Hughes, U. Culha, F. Giardina, F. Guenther, A. Rosendo, and F. Iida, "Soft manipulators and grippers: A review," *Frontiers in Robotics and AI*, vol. 3, Art. no. 69, 2016, doi: 10.3389/frobt.2016.00069.

[5] D. Rus and M. T. Tolley, "Design, fabrication and control of soft robots," *Nature*, vol. 521, no. 7553, pp. 467–475, 2015, doi: 10.1038/nature14543.

[6] R. Sahli, G. Pallares, C. Ducottet, I. E. Ben Ali, S. Al Akhrass, M. Guibert, and J. Scheibert, "Evolution of real contact area under shear and the value of static friction of soft materials," *Proceedings of the National Academy of Sciences of the United States of America*, vol. 115, no. 3, pp. 471–476, 2018, doi: 10.1073/pnas.1706434115.

[7] K. Vorvolakos and M. K. Chaudhury, "The effects of molecular weight and temperature on the kinetic friction of silicone rubbers," *Langmuir*, vol. 19, no. 17, pp. 6778–6787, 2003, doi: 10.1021/la027061q.

[8] A. Chateauminois and C. Fretigny, "Local friction at a sliding interface between an elastomer and a rigid spherical probe," *The European Physical Journal E*, vol. 27, no. 2, pp. 221–227, 2008, doi: 10.1140/epje/i2008-10376-5.

[9] B. J. Briscoe and D. Tabor, "The effect of pressure on the frictional properties of polymers," *Wear*, vol. 34, no. 1, pp. 29–38, 1975, doi: 10.1016/0043-1648(75)90306-3.

[10] M. J. Adams, S. A. Johnson, P. Lefèvre, V. Lévesque, V. Hayward, T. André, and J.-L. Thonnard, "Finger pad friction and its role in grip and touch," *Journal of The Royal Society Interface*, vol. 10, no. 80, Art. no. 20120467, 2013, doi: 10.1098/rsif.2012.0467.

[11] N. Xydas and I. Kao, "Modeling of contact mechanics and friction limit surfaces for soft fingers in robotics, with experimental results," *The International Journal of Robotics Research*, vol. 18, no. 9, pp. 941–950, 1999, doi: 10.1177/02783649922066673.

[12] I. Kao and F. Yang, "Stiffness and contact mechanics for soft fingers in grasping and manipulation," *IEEE Transactions on Robotics and Automation*, vol. 20, no. 1, pp. 132–135, 2004, doi: 10.1109/TRA.2003.820868.

[13] J. Kerr and B. Roth, "Analysis of multifingered hands," *The International Journal of Robotics Research*, vol. 4, no. 4, pp. 3–17, 1986, doi: 10.1177/027836498600400401.

[14] M. R. Cutkosky, "On grasp choice, grasp models, and the design of hands for manufacturing tasks," *IEEE Transactions on Robotics and Automation*, vol. 5, no. 3, pp. 269–279, 1989, doi: 10.1109/70.34763.

[15] H. Kinoshita, L. Bäckström, J. R. Flanagan, and R. S. Johansson, "Tangential torque effects on the control of grip forces when holding objects with a precision grip," *Journal of Neurophysiology*, vol. 78, no. 3, pp. 1619–1630, 1997, doi: 10.1152/jn.1997.78.3.1619.

[16] A. W. Goodwin, P. Jenmalm, and R. S. Johansson, "Control of grip force when tilting objects: Effect of curvature of grasped surfaces and applied tangential torque," *The Journal of Neuroscience*, vol. 18, no. 24, pp. 10724–10734, 1998, doi: 10.1523/JNEUROSCI.18-24-10724.1998.

[17] J. R. Flanagan and A. M. Wing, "The role of internal models in motion planning and control: Evidence from grip force adjustments during movements of hand-held loads," *The Journal of Neuroscience*, vol. 17, no. 4, pp. 1519–1528, 1997, doi: 10.1523/JNEUROSCI.17-04-01519.1997.

[18] S. Goyal, A. Ruina, and J. Papadopoulos, "Planar sliding with dry friction Part 1. Limit surface and moment function," *Wear*, vol. 143, no. 2, pp. 307–330, 1991, doi: 10.1016/0043-1648(91)90104-3.

[19] R. D. Howe and M. R. Cutkosky, "Practical force-motion models for sliding manipulation," *The International Journal of Robotics Research*, vol. 15, no. 6, pp. 557–572, 1996, doi: 10.1177/027836499601500603.

[20] B. N. J. Persson, "Theory of rubber friction and contact mechanics," *The Journal of Chemical Physics*, vol. 115, no. 8, pp. 3840–3861, 2001, doi: 10.1063/1.1388626.

[21] S. Macfarlane and E. A. Croft, "Jerk-bounded manipulator trajectory planning: Design for real-time applications," *IEEE Transactions on Robotics and Automation*, vol. 19, no. 1, pp. 42–52, 2003, doi: 10.1109/TRA.2002.807548.

[22] A. Gasparetto and V. Zanotto, "A technique for time-jerk optimal planning of robot trajectories," *Robotics and Computer-Integrated Manufacturing*, vol. 24, no. 3, pp. 415–426, 2008, doi: 10.1016/j.rcim.2007.04.001.

[23] M. Costanzo, G. De Maria, and C. Natale, "Two-fingered in-hand object handling based on force/tactile feedback," *IEEE Transactions on Robotics*, vol. 36, no. 1, pp. 157–173, 2020, doi: 10.1109/TRO.2019.2944130.

[24] M. Costanzo, "Control of robotic object pivoting based on tactile sensing," *Mechatronics*, vol. 76, Art. no. 102545, 2021, doi: 10.1016/j.mechatronics.2021.102545.

[25] S. M. Kargar and G. Berselli, "Enhancing gripping stability for delicate object handling: Frictional insights into textured soft pads," *The International Journal of Advanced Manufacturing Technology*, vol. 140, no. 11–12, pp. 6413–6424, 2025, doi: 10.1007/s00170-025-16625-1.

[26] M. Buss, H. Hashimoto, and J. B. Moore, "Dextrous hand grasping force optimization," *IEEE Transactions on Robotics and Automation*, vol. 12, no. 3, pp. 406–418, 1996, doi: 10.1109/70.499823.

[27] K. B. Shimoga, "Robot grasp synthesis algorithms: A survey," *The International Journal of Robotics Research*, vol. 15, no. 3, pp. 230–266, 1996, doi: 10.1177/027836499601500302.

[28] M. A. Roa and R. Suárez, "Grasp quality measures: Review and performance," *Autonomous Robots*, vol. 38, no. 1, pp. 65–88, 2015, doi: 10.1007/s10514-014-9402-3.

[29] M. R. Cutkosky and P. K. Wright, "Friction, stability and the design of robotic fingers," *The International Journal of Robotics Research*, vol. 5, no. 4, pp. 20–37, 1986, doi: 10.1177/027836498600500402.

[30] A. Bicchi, "Hands for dexterous manipulation and robust grasping: A difficult road toward simplicity," *IEEE Transactions on Robotics and Automation*, vol. 16, no. 6, pp. 652–662, 2000, doi: 10.1109/70.897777.

[31] T. Inoue and S. Hirai, "Elastic model of deformable fingertip for soft-fingered manipulation," *IEEE Transactions on Robotics*, vol. 22, no. 6, pp. 1273–1279, 2006, doi: 10.1109/TRO.2006.886274.

[32] R. D. Mindlin, "Compliance of elastic bodies in contact," *Journal of Applied Mechanics*, vol. 16, no. 3, pp. 259–268, 1949, doi: 10.1115/1.4009973.

[33] S. Goyal, A. Ruina, and J. Papadopoulos, "Planar sliding with dry friction Part 2. Dynamics of motion," *Wear*, vol. 143, no. 2, pp. 331–352, 1991, doi: 10.1016/0043-1648(91)90105-4.

[34] J. Zhou, M. T. Mason, R. Paolini, and D. Bagnell, "A convex polynomial model for planar sliding mechanics: Theory, application, and experimental validation," *The International Journal of Robotics Research*, vol. 37, no. 2–3, pp. 249–265, 2018, doi: 10.1177/0278364918755536.

[35] K. L. Johnson, K. Kendall, and A. D. Roberts, "Surface energy and the contact of elastic solids," *Proceedings of the Royal Society of London. A. Mathematical and Physical Sciences*, vol. 324, no. 1558, pp. 301–313, 1971, doi: 10.1098/rspa.1971.0141.

[36] S. E. Tomlinson, R. Lewis, and M. J. Carré, "Review of the frictional properties of finger-object contact when gripping," *Proceedings of the Institution of Mechanical Engineers, Part J: Journal of Engineering Tribology*, vol. 221, no. 8, pp. 841–850, 2007, doi: 10.1243/13506501JET313.

[37] S. Derler and L.-C. Gerhardt, "Tribology of skin: Review and analysis of experimental results for the friction coefficient of human skin," *Tribology Letters*, vol. 45, no. 1, pp. 1–27, 2012, doi: 10.1007/s11249-011-9854-y.

[38] B. M. Dzidek, M. J. Adams, J. W. Andrews, Z. Zhang, and S. A. Johnson, "Contact mechanics of the human finger pad under compressive loads," *Journal of The Royal Society Interface*, vol. 14, no. 127, Art. no. 20160935, 2017, doi: 10.1098/rsif.2016.0935.

[39] I. D. Johnston, D. K. McCluskey, C. K. L. Tan, and M. C. Tracey, "Mechanical characterization of bulk Sylgard 184 for microfluidics and microengineering," *Journal of Micromechanics and Microengineering*, vol. 24, no. 3, Art. no. 035017, 2014, doi: 10.1088/0960-1317/24/3/035017.

[40] L. Marechal, P. Balland, L. Lindenroth, F. Petrou, C. Kontovounisios, and F. Bello, "Toward a common framework and database of materials for soft robotics," *Soft Robotics*, vol. 8, no. 3, pp. 284–297, 2021, doi: 10.1089/soro.2019.0115.

[41] W. Chen, H. Khamis, I. Birznieks, N. F. Lepora, and S. J. Redmond, "Tactile sensors for friction estimation and incipient slip detection—Toward dexterous robotic manipulation: A review," *IEEE Sensors Journal*, vol. 18, no. 22, pp. 9049–9064, 2018, doi: 10.1109/JSEN.2018.2868340.

[42] R. A. Romeo and L. Zollo, "Methods and sensors for slip detection in robotics: A survey," *IEEE Access*, vol. 8, pp. 73027–73050, 2020, doi: 10.1109/ACCESS.2020.2987849.

[43] M. Pellicciari, G. Berselli, F. Leali, and A. Vergnano, "A method for reducing the energy consumption of pick-and-place industrial robots," *Mechatronics*, vol. 23, no. 3, pp. 326–334, 2013, doi: 10.1016/j.mechatronics.2013.01.013.